frontiers in Microbiology

ORIGINAL RESEARCH
published: 29 September 2020
doi: 10.3389/fmicb.2020.572331

Genomic Modeling as an Approach to Identify Surrogates for Use in Experimental Validation of SARS-CoV-2 and HuNoV Inactivation by UV-C Treatment

Brahmaiah Pendyala[1], Ankit Patras[1]*, Bharat Pokharel[1] and Doris D'Souza[2]*

[1] Department of Agricultural and Environmental Sciences, Food Science Program, College of Agriculture, Tennessee State University, Nashville, TN, United States, [2] Department of Food Science, University of Tennessee, Knoxville, Knoxville, TN, United States

OPEN ACCESS

Edited by:
Mirian A. F. Hayashi,
Federal University of São Paulo, Brazil

Reviewed by:
Anca Ioana Nicolau,
Dunarea de Jos University, Romania
Kalmia Kniel,
University of Delaware, United States

****Correspondence:***
Ankit Patras
apatras@tnstate.edu
Brahmaiah Pendyala
bpendyal@tnstate.edu

Specialty section:
This article was submitted to Antimicrobials, Resistance and Chemotherapy, a section of the journal Frontiers in Microbiology

Received: *13 June 2020*
Accepted: *08 September 2020*
Published: *29 September 2020*

Citation:
Pendyala B, Patras A, Pokharel B and D'Souza D (2020) Genomic Modeling as an Approach to Identify Surrogates for Use in Experimental Validation of SARS-CoV-2 and HuNoV Inactivation by UV-C Treatment. Front. Microbiol. 11:572331. doi: 10.3389/fmicb.2020.572331

Severe Acute Respiratory Syndrome coronavirus-2 (SARS-CoV-2) is responsible for the COVID-19 pandemic that continues to pose significant public health concerns. While research to deliver vaccines and antivirals are being pursued, various effective technologies to control its environmental spread are also being targeted. Ultraviolet light (UV-C) technologies are effective against a broad spectrum of microorganisms when used even on large surface areas. In this study, we developed a pyrimidine dinucleotide frequency based genomic model to predict the sensitivity of select enveloped and non-enveloped viruses to UV-C treatments in order to identify potential SARS-CoV-2 and human norovirus surrogates. The results revealed that this model was best fitted using linear regression with r^2 = 0.90. The predicted UV-C sensitivity (D_{90} – dose for 90% inactivation) for SARS-CoV-2 and MERS-CoV was found to be 21.5 and 28 J/m^2, respectively (with an estimated 18 J/m^2 obtained from published experimental data for SARS-CoV-1), suggesting that coronaviruses are highly sensitive to UV-C light compared to other ssRNA viruses used in this modeling study. Murine hepatitis virus (MHV) A59 strain with a D_{90} of 21 J/m^2 close to that of SARS-CoV-2 was identified as a suitable surrogate to validate SARS-CoV-2 inactivation by UV-C treatment. Furthermore, the non-enveloped human noroviruses (HuNoVs), had predicted D_{90} values of 69.1, 89, and 77.6 J/m^2 for genogroups GI, GII, and GIV, respectively. Murine norovirus (MNV-1) of GV with a D_{90} = 100 J/m^2 was identified as a potential conservative surrogate for UV-C inactivation of these HuNoVs. This study provides useful insights for the identification of potential non-pathogenic (to humans) surrogates to understand inactivation kinetics and their use in experimental validation of UV-C disinfection systems. This approach can be used to narrow the number of surrogates used in testing UV-C inactivation of other human and animal ssRNA viral pathogens for experimental validation that can save cost, labor and time.

Keywords: genomic modeling, UV-C inactivation, viruses, SARS-CoV-2 (2019-nCoV), norovirus (NoV), surrogates

INTRODUCTION

Coronaviruses belong to the family of *Coronaviridae*, comprising of 26 to 30 kb, positive-sense, single-stranded RNA, in an enveloped capsid (Woo et al., 2010). Coronaviruses can cause severe infectious diseases in human and vertebrates, being fatal in some cases. Severe acute respiratory syndrome (SARS) coronavirus (SARS-CoV-1), a β-coronavirus emerged in Guangdong, southern China, in November, 2002 (Guan et al., 2003), and the Middle East respiratory syndrome (MERS) coronavirus (MERS-CoV), was first detected in Saudi Arabia in 2012 (Alagaili et al., 2014). Since late December 2019, a novel β-coronavirus (2019-nCoV or SARS-CoV-2) has been responsible for the pandemic coronavirus disease (COVID-19) with >7.2 million confirmed cases throughout the world, and a fatality rate of approximately 5.7% as of 11 June, 2020 (World Health Organization [WHO], 2020a). This 2019-nCoV is thought to have originated from a seafood market of Wuhan city, Hubei province, China, and has spread rapidly to other provinces of China and other countries (Zhu et al., 2020).

According to current evidence documented by the World Health Organization [WHO] (2020a,b), SARS-CoV-2 virus (2019-nCoV) is transmitted between humans through respiratory droplets and contact (person-to-person, fomites, etc.) routes (World Health Organization [WHO], 2020b). van Doremalen et al. (2020) reported that SARS-CoV-2 remained viable in aerosols throughout the 3 h duration of the experiment and more stable on plastic and stainless steel than on copper and cardboard, and virus was detected up to 72 h after the application to these surfaces at 21–23°C and 40% relative humidity. Given the ability of these viruses to survive in the environment, appropriate treatment strategies are needed to inactivate SARS-CoV-2. As per WHO recommendations, SARS-CoV-2 may be inactivated using chemical disinfectants. As of 07 April, 2020, the United States Environmental Protection Agency [USEPA] (2020) has announced a list of 428 registered chemical disinfectants that have been approved for use against SARS-CoV-2 (United States Environmental Protection Agency [USEPA], 2020). On the other hand, physical disinfection method "ultraviolet light (UV) treatment" (with germicidal UV-C at wavelengths from 100 to 280 nm) can be an effective approach to inactivate SARS-CoV-2 on surface areas and in the air. UV inactivates a broad spectrum of microorganisms by damaging the DNA or RNA and thereby prevents and/or alters cellular functions and replication (Patras et al., 2020). UV-C inactivation of various microorganisms such as pathogenic bacteria, spores, protozoa, algae and viruses has been reported (Malayeri et al., 2016; Bhullar et al., 2019; Gopisetty et al., 2019; Pendyala et al., 2019, 2020; Patras et al., 2020). Because UV inactivation studies with SARS-CoV-2 requires specifically trained and skilled personnel working under biosafety level 3 (BSL-3) laboratory containment conditions, the use of surrogate coronaviruses has the potential to cross these hurdles for experimental validation of designed UV systems. Based on the biophysical properties and genomic structure, literature studies on testing the efficacy of disinfectants against coronaviruses used the following surrogates; murine hepatitis virus (MHV), Human coronavirus 229 E, transmissible gastroenteritis virus (TGEV), and feline infectious peritonitis virus (FIPV) (Kumar et al., 2020). However, the selection of potential surrogates to SARS-CoV-2 requires a comparative evaluation of UV-C sensitivity between these viruses. As of date, the precise experimental UV-C susceptibility (D_{90} value) of SARS-CoV/SARS-CoV-2 is not reported.

Human noroviruses (HuNoVs) cause >80% of global non-bacterial gastroenteritis that can be spread through contamination of food, water, fomites, or direct contact, and also via aerosolization (Fankhauser et al., 2002; Widdowson et al., 2005; Godoy et al., 2006). HuNoVs are also single-stranded RNA viruses that are small 27 to 32 nM in size that belong to the *Caliciviridae* family. However, HuNoVs are enclosed in a non-enveloped capsid, unlike SARS-CoV-2 that is enveloped. UV-C inactivation data on the HuNoV genogroups is limited due to the lack of available cultivation methods to obtain high infectious titers (Doultree et al., 1999; Ettayebi et al., 2016; Estes et al., 2019). Thus, reverse transcription quantitative polymerase chain reaction (RT-qPCR) is widely used for assessing survivor populations of HuNoVs after treatment. However, research studies showed overestimation of survivors with RT-qPCR in comparison to virus infectivity plaque assays (Rönnqvist et al., 2014; Wang and Tian, 2013; Walker et al., 2019). As an alternative, cultivable animal viruses [caliciviruses, echoviruses and murine norovirus (MNV)] have been used as surrogates to determine UV-C inactivation of HuNoVs (Thurston-Enriquez et al., 2003; de Roda Husman et al., 2004; Lee et al., 2008; Park et al., 2011), but proper selection of surrogates which mimic the UV-C inactivation characteristics of HuNoVs is required to evaluate kinetics and scale up validation studies.

Furthermore, it is well known that microorganisms respond to UV exposure at rates defined in terms of UV rate constants (Patras et al., 2020). The slope of the logarithmic decay curve is defined by the rate constant, which is designated as k. The UV rate constant k has units of cm^2/mJ or m^2/J and is also known as the UV susceptibility. It can be also defined as D_{90} or D_{10} [dose for 90% inactivation or 10% survival] as the primary indicator of UV susceptibility. UV dose is expressed as J/m^2 or mJ/cm^2 (Patras et al., 2020). The varied microbial sensitivity to ultraviolet light (UV) among species of microbes, is due to several intrinsic factors including physical size, presence of chromophores or UV absorbers, presence of repair enzymes or dark/light repair mechanisms, hydrophilic surface properties, relative index of refraction, specific UV spectrum (broad band UVC/UVB versus narrow band UVC), genome based parameters; molecular weight of nucleic acids, DNA conformation (A or B), G+C%, and % of potential pyrimidine or purine dimerization (Kowalski et al., 2009).

The physical size of a virus bears no clear relationship with UV susceptibility, except that for the largest viruses, as size increases, the UV rate constant tends to decrease slightly (which is likely the result of UV scattering) (Kowalski et al., 2009). There is no thorough literature available on the above-mentioned optical parameters, hydrophilic surface properties and repair mechanisms relating to UV sensitivity. On the other hand, genome sequences of UV susceptibility can be easily retrieved from genome databases and the development of genomic models

based on the above mentioned genome-based parameters is feasible to predict the UV susceptibility of ssRNA viruses, which include human pathogenic novel viruses (such as SARS-CoV-2) and cultivation-challenging HuNoVs.

Our hypothesis is that predicting UV-C inactivation based on genomic modeling, will enable the determination of surrogates to be used in UV-C validation studies. In the present study, we attempted to develop a genomic model to predict and compare the UV sensitivity of enveloped SARS-CoV-2 and non-enveloped HuNoVs and to determine their suitable surrogates for use in UV-C process validation.

MATERIALS AND METHODS

Collection of Reported ssRNA Viruses UV_{254} Sensitivity (D_{90} Values)

We collected UV-C sensitivity of ssRNA viruses form published studies and carefully selected D_{90} values (**Table 1**). The selection was based on the careful assessment of methods that were used to determine UV-C sensitivity. The selected UV-C sensitivity of an ssRNA virus is determined via the standard method (Bolton and Linden, 2003), with the $\log_{10}$ survivors as a function of UV dose and represented as D_{90}.

TABLE 1 | Reported UV sensitivity (D_{90}) data for ssRNA viruses.

Virus	Average D_{90} (J/m^2)	Reference source
Murine sarcoma virus	190	Kelloff et al., 1970; Nomura et al., 1972
Bacteriophage MS2	183[a]	Malayeri et al., 2016
Moloney murine leukemia virus	115	Nomura et al., 1972
Murine norovirus	100	Lee et al., 2008; Park et al., 2011
Coxsackievirus	79	Battigelli et al., 1993; Gerba et al., 2002; Shin et al., 2005
Human parechovirus	75	Gerba et al., 2002
Polio virus	73	Gerba et al., 2002; Thompson et al., 2003; Lazarova and Savoye, 2004; Shin et al., 2005; Simonet and Gantzer, 2006
Canine calicivirus (CCV)	67	de Roda Husman et al., 2004
Feline calicivirus (FCV)	60	Thurston-Enriquez et al., 2003; de Roda Husman et al., 2004; Park et al., 2011
Sindbis virus	55	Zavadova and Libikova, 1975; von Brodorotti and Mahnel, 1982
Venezuelan equine encephalitis virus	55	Smirnov et al., 1992
Western equine encephalomyelitis virus	54	Dubinin et al., 1975
Hepatitis A virus	51	Wilson et al., 1992; Battigelli et al., 1993; Wiedenmann et al., 1993
Semliki forest virus	25	Weiss and Horzinek, 1986
Measles virus	22	Stefano et al., 1976
SARS-CoV-1	18[b]	Kariwa et al., 2006

Average D_{90} values refer average of reference source studies.
[a]Average value of all (45) MS2 reports.
[b]Estimated value from initial linear kinetics of data and considering 90% of light transmission through test fluid.

Determination of Genomic Parameters; Genome Size, and Pyrimidine Dinucleotide Frequency Value (PyNNFV)

The molecular size and nucleotide sequences of genomes used in this study were directly obtained from available NCBI genome database (**Table 2** and **Table 5**). PyNNFV model was developed based on the frequency of each type of pyrimidine dinucleotides (TT, TC, CT, and CC) which varies based on genome sequences. Pyrimidines are almost 10 times more susceptible to photoreaction (Smithyman and Hanawalt, 1969), while strand breaks, inter-strand cross links and DNA-protein cross links form with less frequency (1:1000 of the number of dimers and hydrates) (Setlow and Carrier, 1966). Three simple rules were formulated for sequence-dependent dimerization (Becker and Wang, 1989); "(i) When two or more pyrimidines are neighboring to one another, photoreactions are observed at both pyrimidines, (ii) Non-adjacent pyrimidines exhibit little or no photoreactivity, and (iii) Purines form UV photoproducts when they are flanked at 5′ side by two or more adjacent pyrimidine residues." Therefore, we considered 100% probability of formation of photoreaction products when PyNN are flanked by pyrimidines on both sides and 50% probability when PyNN are flanked by purine on either side. The individual PyNNs were counted by the exclusive method (each pyrimidine considered in one PyNN combination only). Research studies showed the proportion of photoreaction products in the order of TT > TC > CT > CC (Douki, 2013), thus same sequence was followed in counting individual PyNNs. **Table 3** shows the method used for PyNNFV calculation in this study. A mathematical function was written to calculate PyNNFV from the potential PyNNs to exist in the genome of RNA (Eq. 1).

$$\text{PyNNFV} = \frac{(\text{TT\%})(\text{TC\%})(\text{CT\%})(\text{CC\%})}{\text{genome bp}} \quad (1)$$

The PyNNFVs from complete genome sequences of 16 ssRNA viruses and corresponding reported D_{90} values were used to plot a model graph. Then, the correlation between PyNNFVs and D_{90} values was analyzed by fitting the appropriate regression model (linear regression).

RESULTS AND DISCUSSION

Table 1 shows the median D_{90} values collected from UV-C inactivation studies of various ssRNA viruses. The data was selected from the studies conducted with uniform viral suspensions in transparent medium (water or phosphate buffer saline), followed standard method for UV dose calculation (Bolton and Linden, 2003). The D_{90} values reported for ssRNA viruses ranged from 18 J/m^2 for SARS-CoV-1 to 190 J/m^2 for murine sarcoma virus. Genomic parameters; genome size,

TABLE 2 | Genome size and identified pyrimidine dinucleotide values for collected ssRNA viruses.

Virus	NCBI Accession #	Genome (bp)	PyNNFV[a]
Bacteriophage MS2	NC_001417.2	3569	0.00804
Murine sarcoma virus	NC_001502.1	5833	0.00807
Human parechovirus	NC_001897.1	7348	0.00210
Murine norovirus	NC_008311.1	7382	0.00570
Coxsackievirus	KX595291.1	7410	0.00314
Polio virus	NC_002058.3	7440	0.00263
Hepatitis A virus	KP879217.1	7476	0.00209
Feline calicivirus	NC_001481.2	7683	0.00363
Moloney murine leukemia virus	NC_001501.1	8332	0.00598
Canine Calicivirus	NC_004542.1	8513	0.00345
Semliki forest virus	NC_003215.1	11442	0.00141
Venezuelan equine encephalitis virus	NC_001449.1	11444	0.00153
Western equine encephalomyelitis virus	NC_003908.1	11484	0.00151
Sindbis virus	NC_001547.1	11703	0.00149
Measles virus	NC_001498.1	15894	0.00134
SARS-CoV-1	NC_004718.3	29751	0.00067

[a] *Pyrimidine dinucleotide frequency value.*

PyNNFVs of respective viruses were shown in **Table 2**. The values are in the range of 3569 bp to 29751 bp for genomic size; 0.00067–0.00807 for PyNNFV.

Genomic Models to Predict UV-C Sensitivity of ssRNA Viruses

To determine the relationship between genome size and UV-C sensitivity, the D_{90} values were plotted against the genome size of various ssRNA viruses (**Figure 1**). The data were best fitted to log linear regression model with $r^2 = 0.63$. The results revealed that there was a decisive relationship between genome size and UV sensitivity across the range of 3569–29751 bp.

Further to evaluate the influence of base composition and sequence along with genome size on UV-C sensitivity, the D_{90} values were plotted versus PyNNFV (**Figure 2**). Linear regression model was best fitted with $r^2 = 0.90$. Therefore, based on the value of r squared a moderate positive relationship was found between PyNNFV and UV-C sensitivity of the virus. The following linear regression equation shows the correlation between D_{90} values and PyNNFV.

$$y = 19984x + 10.409 \quad (2)$$

Also, to predict the distribution of UV-C sensitivities and estimates of the true population mean using this model, 95% prediction and confidence intervals were shown in **Figure 2**. To confirm the adequacy of the fitted model, studentized residuals versus run order were tested and the residuals were observed to be scattered randomly, suggesting that the variance was constant. It can be indicated from **Figure 3** that predicted values were in close agreement with the experimental values and were found to be not significantly different at $p > 0.05$ using a paired t-test. Despite some variations, results obtained predicted model and actual experimental values showed that the established models reliably predicted the D_{90} value. Therefore, the predictive performance of the established model can be considered acceptable. The applicability of the models was also quantitatively evaluated by comparing the bias and accuracy factors (**Table 4** and Eqs 3 and 4).

TABLE 3 | Calculation of PyNNFV value for SARS-CoV-2.

Parameter	TT	TC	CT	CC
PyNNs[a]	2454	1020	881	535
PyNNs flanked with purine[a]	773 (ATT) 412 (TTA) 530 (GTT) 230 (TTG)	324 (ATC) 250 (TCA) 174 (GTC) 37 (TCG)	298 (ACT) 244 (CTA) 187 (GCT) 91 (CTG)	281 (ACC) 90 (CCA) 84 (GCC) 10 (CCG)
Total PyNNs flanked with purine	1945	785	820	472
PyNNs flanked without purine	509	235	61	63
Probability of each PyNN[b]	1481.5	627.5	471	299
PyNNs(%)[c]	4.956341	2.099294	1.575725	1.000301
Genome size	29891			
PyNNFV	0.000555			

[a] *Values are counted using exclusive method (once one doublet or triplet is located in the genome, it is excluded from participating in other dimers).*
[b] *Overall probability of each PyNN is calculated by considering 50% probability (0.5) for PyNNs flanked with purine and 100% probability (1.0) for PyNNs flanked without purine.*
[c] *PyNNs% was determined by calculating the% of probability of PyNNs in total genome.*

$$AF = 10^{\frac{\sum \log\left|V_P/V_E\right|}{n_e}} \quad (3)$$

$$BF = 10^{\frac{\sum \log\left(V_P/V_E\right)}{n_e}} \quad (4)$$

$$E(\%) = \frac{1}{n_e}\sum_{i=1}^{n}\left|\left|\frac{V_E - V_P}{V_E}\right|\right| \times 100 \quad (5)$$

The average mean deviation (E%) were used to determine the fitting accuracy of data (Eq. 5). Where, n_e is the number of experimental data, V_E is the experimental value and V_P is the predicted value.

In most cases, as shown in **Table 4**, the accuracy factor (AF) values for the genomic model were close to 1.00, except for Measles virus (0.83), Semliki forest virus (0.86). The bias factor (BF) values for the predicted models were also close to 1.00, ranging from 1.02 to 1.21 for the parameter studied. These results clearly indicate that there was a good agreement between predicted and observed D_{90} values. Ross et al. (2000) stated that predictive models ideally would have an AF = BF = 1.00, indicating a perfect model fit where the predicted and actual response values are equal. However, typically, the AF of a fitted model will increase by 0.10–0.15 units for each predictive variable in the model (Ross et al., 2000). Genomic model, as in this study, that forecasts a response may be expected to have AF and BF

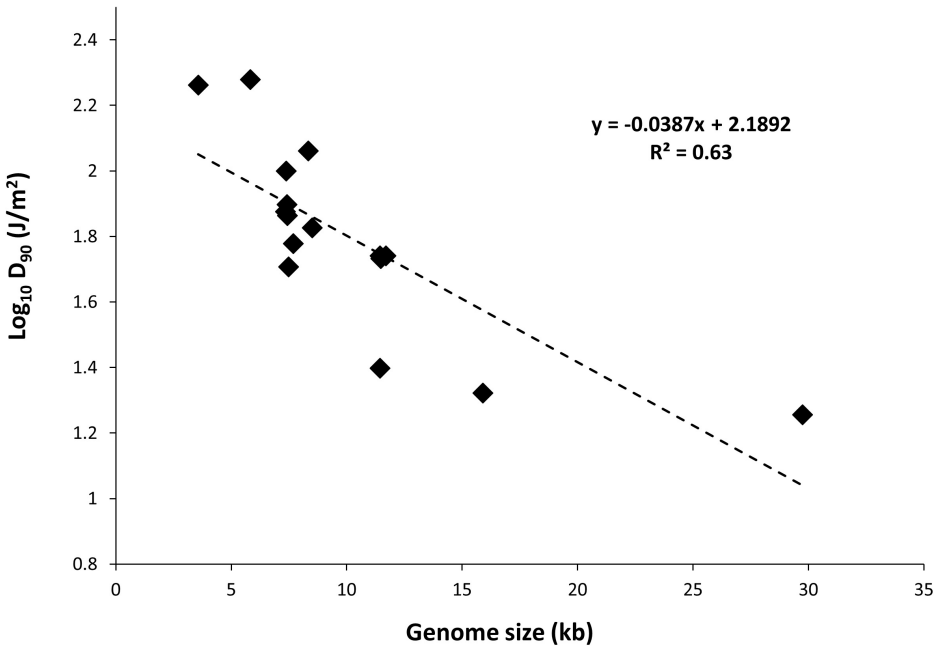

FIGURE 1 | Plot of genome size versus UV-C sensitivity of ssRNA viruses.

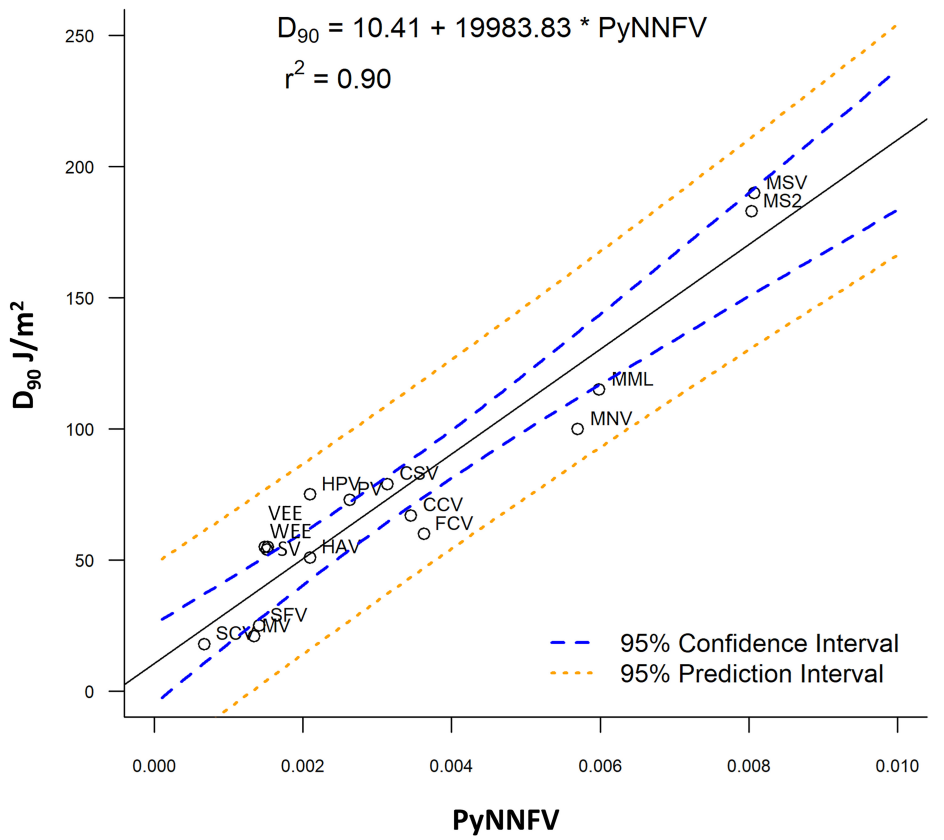

FIGURE 2 | Plot of PyNNFV versus UV-C sensitivity of ssRNA viruses. MSV, murine sarcoma virus; MS2, bacteriophage MS2; MML, moloney murine leukemia virus; CSV, coxsackie virus; HPV, human parechovirus; PV, polio virus; CCV, canine calcivirus; FCV, feline calcivirus; HAV, hepatitis A virus; SV, sindbis virus; VEE, venezuelan equine encephalitis virus; WEE, western equine encephalomyelitis virus; SFV, semliki forest virus; MV, measles virus; SCV, SARS-CoV-1.

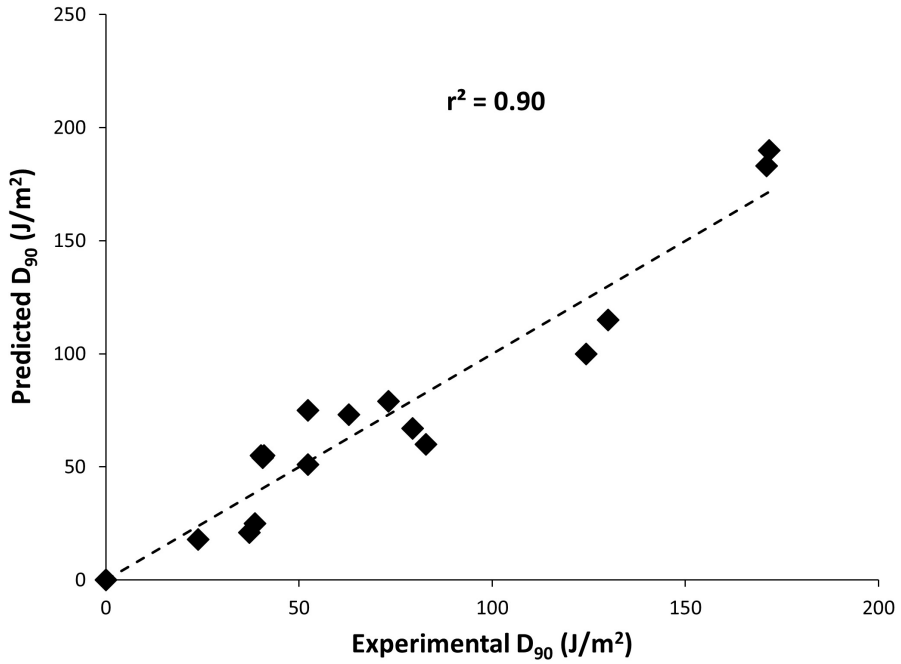

FIGURE 3 | Plot of model predicted D_{90} values versus Experimental D_{90} values.

TABLE 4 | Accuracy factors (AF) and Bias factors (BF) for D_{90} values in the regression analysis.

Virus	AF	BF	E (%)[a]
Bacteriophage MS2	1.02	1.02	2.18
Feline calicivirus	0.9	1.11	12.71
Coxsackievirus	1.03	1.03	2.48
Canine calicivirus	0.94	1.06	6.17
Semliki forest virus	0.86	1.16	18.18
Murine sarcoma	1.03	1.03	3.22
Measles virus	0.83	1.21	25.67
SARS-CoV-1	0.91	1.1	10.88
Murine norovirus	0.93	1.08	8.09
Moloney murine leukemia virus	0.96	1.04	4.33
Human parechovirus	1.13	1.13	10.09
Western equine encephalomyelitis virus	1.1	1.1	8.25
Venezuelan equine encephalitis virus	1.1	1.1	8.55
Sindbis virus	1.11	1.11	9.03
Hepatitis A virus	0.99	1.01	0.82
Polio virus	1.05	1.05	4.62

[a]*Average mean deviation.*

values ranging from 0.83 to 1.21 or an equivalent percentage error range of 0.82–25.67%.

Prediction of UV Sensitivity of Various Corona Viruses and Human Noroviruses

Owing to good model fitting, the PyNNFV genomic model was used to predict UV sensitivity of coronaviruses including SARS-CoV-2 and different HuNoV genogroups. PyNNFV values of target viruses were calculated from genomic sequences obtained from the NCBI database. The UV sensitivities were predicted by substituting PyNNFV value in Eq. 2. **Table 5** shows PyNNFV values and corresponding predicted D_{90} values of target viruses. Predicted D_{90} of SARS-CoV-2 virus (21.5 J/m^2) (**Table 5**) is closer to the estimated D_{90} of SARS-CoV-1 (18 J/m^2) from the experimental study (**Table 1**). Kariwa et al. (2006) irradiated 2 mL of SARS-CoV-1 in 3-cm petri dishes without stirring UV-C light at 134 μW/cm^2 for 15 min, and observed reduction in infectivity from 3.8×10^7 to 180 $TCID_{50}$/mL with equivalent to D_{90} value of 226 J/m^2. In contrast, Darnell et al. (2004) showed 4 log reduction of SARS-CoV-1 at UV-C exposure of 4016 μW/cm^2 for 6 min which is equivalent to D_{90} value of 3610 J/m^2. The authors conducted the experiment in a 24 well plate containing 2 mL virus aliquots without mixing. These two studies neither calculate the average irradiance nor provide conditions for uniform UV-C dose distribution throughout the test fluid and thereby reported higher values. The model predicted D_{90} value of MERS-CoV (28.1 J/m^2) that is found to be higher than SARS-COV-2, whereas murine hepatitis coronavirus (MHV) strains showed similar UV-C sensitivity (D_{90} values = 20.3 to 21 J/m^2). For α- and γ-coronaviruses, the predicted D_{90} values (17.8 to 18.3 J/m^2) were lower than the β-coronaviruses (**Table 5**). Saknimit et al. (1988) demonstrated the efficiency of UV-C irradiation on the inactivation of MHV and CCV coronaviruses using 15 W UV-C lamp at a distance of 1 m and reported efficient UV-C inactivation after 15 min treatment. From this data, the estimated D_{90} values for MHV and CCV (γ-coronavirus) were 17 and 15 J/m^2, respectively, and observed to be slightly lower (∼20%) than the model predicted values (**Table 5**). Overall the results show

TABLE 5 | Predicted of UV sensitivity with respect to dimerization values of target ssRNA viruses.

Virus	NCBI Accession#	Genome (bp)	PyNNF values	Predicted D_{90} Values (J/m^2)
α-coronaviruses				
Transmissible gastroenteritis virus	KX499468.1	28614	0.000391	18.2
Canine coronavirus	KP981644.1	29278	0.000379	18.0 (15.0)
Feline infectious peritonitis virus	KC461237.1	29357	0.000393	18.3
Human coronavirus 229E	KF514433.1	27165	0.000489	20.2
β-coronaviruses				
SARS-CoV-2	MT192772.1	29891	0.000549	21.5
MERS-CoV	MH734115.1	30033	0.000883	28.1
Murine hepatitis virus strain A59	MF618252.1	29947	0.000532	21.0 (17.0)
Murine hepatitis virus strain S	GU593319.1	31147	0.000515	20.7 (17.0)
Murine coronavirus MHV-1	FJ647223.1	31386	0.000526	20.9 (17.0)
Rat coronavirus	JF792617.1	31274	0.000494	20.3
Bat coronavirus BM48-31	NC_014470.1	29276	0.000603	22.5
Bat coronavirus HKU9-1	NC_009021.1	29114	0.000465	19.7
Bat coronavirus HKU4-1	NC_009019.1	30286	0.000580	22.0
Bat Hp-betacoronavirus	NC_025217.1	31491	0.000691	24.2
SARS coronavirus A022 (Civet)	AY686863.1	29499	0.0006401	23.2
SARS coronavirus B039 (Civet)	AY686864.1	29525	0.0006402	23.2
γ-coronavirus				
Avian infectious bronchitis virus	NC_001451.1	27608	0.000371	17.8
Human noroviruses (non-enveloped)				
Norovirus GI	NC_001959.2	7654	0.002936	69.1
Norovirus GII	KF712510.1	7509	0.003934	89.0
Norovirus GIV	JF781268.1	7839	0.00336	77.6

Values in parenthesis denote estimated D_{90} values from experimental study (Saknimit et al., 1988).

that coronaviruses are highly sensitive to UV-C light than other ssRNA viruses reported in **Table 1**. From the UV sensitivity data obtained using the genomic model, it was observed that UV doses ranging from 90 to 141 J/m^2 are required for 5 log reduction of human pathogenic coronaviruses (SARS-CoV-1, MERS-CoV, 2019-nCoV). Here we demonstrate an example of UV exposure using a low-pressure mercury lamp. If the UV-C lamp source provides an average irradiance of 0.4 mW/cm^2 or 4 W/m^2 (under uniform dose distribution conditions), a mere 35 s treatment is adequate to inactivate β-coronaviruses (99.999% or 5 log reduction). Since the developed model relies on total PyNNFV (not on specific gene sequences), slight viral mutations should not cause significant variations in UV sensitivity. For instance, if the PyNNFV value of SARS-CoV-2 changes up to ±10%, the model predicted UV sensitivity (D_{90} value) ranges from 20.4 to 22.6 J/m^2 with the change of just ±2.6%.

The predicted D_{90} values of HuNoVs are 69.1, 89, and 77.6 J/m^2 for genogroups, GI, GII, and GIV, respectively (**Table 5**). The results revealed that the UV-C sensitivity of GII was lower with higher predicted D_{90} value in comparison to GI and GIV. To the best of our knowledge, limited experimental data is currently available on UV-C sensitivity of HuNoVs. Some research studies used RT-qPCR method to estimate MNV survivors and validated with virus infectivity assay (Wang and Tian, 2013; Rönnqvist et al., 2014; Walker et al., 2019). The reported validation results showed that the values obtained with RT-qPCR method are overestimated compared to standard virus infectivity assays (Wang and Tian, 2013; Rönnqvist et al., 2014; Walker et al., 2019). For instance, Rönnqvist et al. (2014) reported 4-log reduction of MNV at a UV dose of 60 mJ/cm^2 with the infectivity assay, whereas just 2-log decline of MNV and HuNoV RNA levels was found at a UV dose of 150 mJ/cm^2 by the RT-qPCR method. The experimental D_{90} values of conservative surrogates (MNV, echovirus and caliciviruses) obtained via viability assay are reported to be in the range of 60–100 J/m^2 (**Table 1**).

Identification of Potential Surrogates for UV-C Inactivation

Validation of the UV-C inactivation kinetics of specific pathogens such as SARS-CoV-2 is not possible (without the use of appropriate surrogates) because of the need for sophisticated biosafety level (BSL)-3 containment, and to protect the researchers, and the public from health risk in environmental settings. For HuNoV, research on reproducible cultivable systems that obtain high titers are still on-going. Hence, criteria for the selection and application of surrogates are required to ensure that the surrogates mimic the behavior of the SARS-CoV-2 or HuNoVs under specific treatment conditions, while ensuring safety of personnel and also decreasing labor, cost and time. Also, surrogates are useful in process validation studies

at scale up that can reduce the uncertainties linked with UV-C dose measurement.

As seen from **Table 5**, the model predicted D_{90} value (∼21.5 J/m^2) of SARS-CoV-2 was comparable to MHV strains (non-pathogenic to humans) of the β-coronavirus group (∼21 J/m^2), higher than α-coronaviruses (TGEV, CCV, and FIPV) and γ-coronavirus (AIBV) (∼18 J/m^2). Also, since both SARS-CoV-2 and MHV are β-coronaviruses, MHV-strain A59 may show similar behavior under various culture conditions making it a potential surrogate for SARS-CoV-2 for UV-C inactivation kinetics and validation studies.

For HuNoVs, the predicted D_{90} values of all genogroups (69–89 J/m^2) were higher than D_{90} values of the reported caliciviruses (60–67 J/m^2) in our study, echoviruses (75 J/m^2), except being lower than MNV-1 (100 J/m^2) (**Tables 1**, **5**). Use of surrogates that exhibit similar or slightly higher D_{90} values to target pathogens can avoid the risk associated with improper inactivation, hence our results indicate that MNV-1 is the better choice (though conservative) to validate UV-C inactivation of all HuNoVs under laboratory experimental setup conditions.

In conclusion, a predictive genomic-modeling method was developed for estimating the UV sensitivity of SARS-CoV-2 and HuNoVs. Results of the model validation showed that the developed model had acceptable predictive performance, as assessed by mathematical and graphical model performance indices. We predicted the $\boldsymbol{D}_{90}$ values by conducting extensive genomic modeling. Although the parameters reported here may suffice to estimate the UV sensitivity, experimental research directed to address various knowledge gaps identified in this study is required to maximize the accuracy of predicted models. Additional parameters will be computed to the predictive model as needed, including terms for the presence of chromophores or UV absorbers and for possible UV scattering.

DATA AVAILABILITY STATEMENT

All datasets presented in this study are included in the article/supplementary material.

AUTHOR CONTRIBUTIONS

BPe and AP conceived of the presented idea and wrote the manuscript. BPe developed the theory and performed the computations. BPo contributed to statistical analysis. BPe, AP, and DD'S contributed to the interpretation and discussion of the results. All authors contributed to the article and approved the submitted version.

FUNDING

This project is funded under the Agriculture and Food Research Initiative (Food Safety Challenge Area), USDA, Award numbers; 2018-38821-27732 and 2019-69015-29233.

REFERENCES

Alagaili, A. N., Briese, T., Mishra, N., Kapoor, V., Sameroff, S. C., Burbelo, P. D., et al. (2014). Middle east respiratory syndrome coronavirus infection in dromedary camels in Saudi Arabia. *mBio* 5:e00884-14. doi: 10.1128/mBio.00884-14

Battigelli, D. A., Sobsey, M. D., and Lobe, D. C. (1993). The inactivation of hepatitis A virus and other model viruses by UV irradiation. *Water Sci. Technol.* 27, 339–342. doi: 10.2166/wst.1993.0371

Becker, M. M., and Wang, Z. (1989). Origin of ultraviolet damage in DNA. *J. Mol. Biol.* 210, 429–438. doi: 10.1016/0022-2836(89)90120-4

Bhullar, M. S., Patras, A., Kilonzo-Nthenge, A., Pokharel, B., and Sasges, M. (2019). Ultraviolet inactivation of bacteria and model viruses in coconut water using a collimated beam system. *Food Sci. Technol. Int.* 25, 562–572. doi: 10.1177/1082013219843395

Bolton, J. R., and Linden, K. G. (2003). Standardization of methods for fluence (UV dose) determination in bench-scale UV experiments. *J. Environ. Eng.* 129, 209–215. doi: 10.1061/(asce)0733-9372(2003)129:3(209)

Darnell, M. E., Subbarao, K., Feinstone, S. M., and Taylor, D. R. (2004). Inactivation of the coronavirus that induces severe acute respiratory syndrome, SARS-CoV. *J. Virol. Methods* 121, 85–91. doi: 10.1016/j.jviromet.2004.06.006

de Roda Husman, A. M., Bijkerk, P., Lodder, W., Van Den Berg, H., Pribil, W., Cabaj, A., et al. (2004). Calicivirus inactivation by nonionizing (253.7-nanometer-wavelength [UV]) and ionizing (gamma) radiation. *Appl. Environ. Microbiol.* 70, 5089–5093. doi: 10.1128/aem.70.9.5089-5093.2004

Douki, T. (2013). The variety of UV-induced pyrimidine dimeric photoproducts in DNA as shown by chromatographic quantification methods. *Photochem. Photobiol. Sci.* 12, 1286–1302. doi: 10.1039/c3pp25451h

Doultree, J. C., Druce, J. D., Birch, C. J., Bowden, D. S., and Marshall, J. A. (1999). Inactivation of feline calicivirus, a Norwalk virus surrogate. *J. Hosp. Infect.* 41, 51–57. doi: 10.1016/s0195-6701(99)90037-3

Dubinin, N. P., Zasukhina, G. D., Nesmashnova, V. A., and Lvova, G. N. (1975). Spontaneous and induced mutagenesis in western equine encephalomyelitis virus in chick embryo cells with different repair activity. *Proc. Natl. Acad. Sci. U.S.A.* 72, 386–388. doi: 10.1073/pnas.72.1.386

Estes, M. K., Ettayebi, K., Tenge, V. R., Murakami, K., Karandikar, U., Lin, S. C., et al. (2019). Human norovirus cultivation in nontransformed stem cell-derived human intestinal enteroid cultures: success and challenges. *Viruses* 11, 638. doi: 10.3390/v11070638

Ettayebi, K., Crawford, S. E., Murakami, K., Broughman, J. R., Karandikar, U., Tenge, V. R., et al. (2016). Replication of human noroviruses in stem cell–derived human enteroids. *Science* 353, 1387–1393. doi: 10.1126/science.aaf5211

Fankhauser, R. L., Monroe, S. S., Noel, J. S., Humphrey, C. D., Bresee, J. S., Parashar, U. D., et al. (2002). Epidemiologic and molecular trends of "Norwalk-like viruses" associated with outbreaks of gastroenteritis in the United States. *J. Infect. Dis.* 186, 1–7. doi: 10.1086/341085

Gerba, C. P., Gramos, D. M., and Nwachuku, N. (2002). Comparative inactivation of enteroviruses and adenovirus 2 by UV light. *Appl. Environ. Microbiol.* 68, 5167–5169. doi: 10.1128/aem.68.10.5167-5169.2002

Godoy, P., Nuin, C., Alseda, M., Llovet, T., Mazana, R., and Dominguez, A. (2006). Waterborne outbreak of gastroenteritis caused by Norovirus transmitted through drinking water. *Rev. Clin. Esp.* 206, 435–437.

Gopisetty, V. V. S., Patras, A., Pendyala, B., Kilonzo-Nthenge, A., Ravi, R., Pokharel, B., et al. (2019). UV-C irradiation as an alternative treatment technique: study of its effect on microbial inactivation, cytotoxicity, and sensory properties in cranberry-flavored water. *Innov. Food Sci. Emerg.* 52, 66–74. doi: 10.1016/j.ifset.2018.11.002

Guan, Y., Zheng, B. J., He, Y. Q., Liu, X. L., Zhuang, Z. X., Cheung, C. L., et al. (2003). Isolation and characterization of viruses related to the SARS coronavirus from animals in southern China. *Science* 302, 276–278. doi: 10.1126/science.1087139

Kariwa, H., Fujii, N., and Takashima, I. (2006). Inactivation of SARS coronavirus by means of povidone-iodine, physical conditions and chemical reagents. *Dermatology* 212, 119–123. doi: 10.1159/000089211

Kelloff, G., Aaronson, S. A., and Gilden, R. V. (1970). Inactivation of murine sarcoma and leukemia viruses by ultra-violet irradiation. *Virology* 42, 1133–1135. doi: 10.1016/0042-6822(70)90361-2

Kowalski, W. J., Bahnfleth, W. P., and Hernandez, M. T. (2009). A genomic model for the prediction of ultraviolet inactivation rate constants for RNA and DNA viruses. *IUVA News* 11, 15–28.

Kumar, G. D., Mishra, A., Dunn, L., Townsend, A., Oguadinma, I. C., Bright, K. R., et al. (2020). Biocides and novel antimicrobial agents for the mitigation of coronaviruses. *Front. Microbiol.* 11:1351. doi: 10.3389/fmicb.2020.01351

Lazarova, V., and Savoye, P. (2004). Technical and sanitary aspects of wastewater disinfection by UV irradiation for landscape irrigation. *Water Sci. Technol.* 50, 203–209. doi: 10.2166/wst.2004.0125

Lee, J., Zoh, K., and Ko, G. (2008). Inactivation and UV disinfection of murine norovirus with TiO2 under various environmental conditions. *Appl. Environ. Microbiol.* 74, 2111–2117. doi: 10.1128/aem.02442-07

Malayeri, A. H., Mohseni, M., Cairns, B., Bolton, J. R., Chevrefils, G., Caron, E., et al. (2016). Fluence (UV dose) required to achieve incremental log inactivation of bacteria, protozoa, viruses and algae. *IUVA News* 18, 4–6.

Nomura, S., Bassin, R. H., Turner, W., Haapala, D. K., and Fischinger, P. J. (1972). Ultraviolet inactivation of Moloney leukaemia virus: relative target size required for virus replication and rescue of 'defective' murine sarcoma virus. *J. Gen. Virol.* 14, 213–217. doi: 10.1099/0022-1317-14-2-213

Park, G. W., Linden, K. G., and Sobsey, M. D. (2011). Inactivation of murine norovirus, feline calicivirus and echovirus 12 as surrogates for human norovirus (NoV) and coliphage (F+) MS2 by ultraviolet light (254 nm) and the effect of cell association on UV inactivation. *Lett. Appl. Microbiol.* 52, 162–167. doi: 10.1111/j.1472-765x.2010.02982.x

Patras, A., Bhullar, M. S., Pendyala, B., and Crapulli, F. (2020). *Ultraviolet Treatment of Opaque Liquid Foods: From Theory to Practice. Reference Module in Food Science*. Amsterdam: Elsevier.

Pendyala, B., Patras, A., Gopisetty, V. V. S., Sasges, M., and Balamurugan, S. (2019). Inactivation of Bacillus and Clostridium spores in coconut water by ultraviolet light. *Foodborne Pathog. Dis.* 16, 704–711. doi: 10.1089/fpd.2019.2623

Pendyala, B., Patras, A., Ravi, R., Gopisetty, V. V. S., and Sasges, M. (2020). Evaluation of UV-C irradiation treatments on microbial safety, ascorbic acid, and volatile aromatics content of watermelon beverage. *Food Bioprocess Technol.* 13, 101–111. doi: 10.1007/s11947-019-02363-2

Rönnqvist, M., Mikkelä, A., Tuominen, P., Salo, S., and Maunula, L. (2014). Ultraviolet light inactivation of murine norovirus and human norovirus GII: PCR may overestimate the persistence of noroviruses even when combined with pre-PCR treatments. *Food Environ. Virol.* 6, 48–57. doi: 10.1007/s12560-013-9128-y

Ross, T., Dalgaard, P., and Tienungoon, S. (2000). Predictive modelling of the growth and survival of Listeria in fishery products. *Int. J. Food Microbiol.* 62, 231–245. doi: 10.1016/s0168-1605(00)00340-8

Saknimit, M., Inatsuki, I., Sugiyama, Y., and Yagami, K. I. (1988). Virucidal efficacy of physico-chemical treatments against coronaviruses and parvoviruses of laboratory animals. *Exp. Anim.* 37, 341–345. doi: 10.1538/expanim1978.37.3_341

Setlow, R., and Carrier, W. L. (1966). Pyrimidine dimers in ultraviolet-irradiated DNA's. *J. Mol. Biol.* 17, 237–254. doi: 10.1016/s0022-2836(66)80105-5

Shin, G. A., Linden, K. G., and Sobsey, M. D. (2005). Low pressure ultraviolet inactivation of pathogenic enteric viruses and bacteriophages. *J. Environ. Eng. Sci.* 4, S7–S11.

Simonet, J., and Gantzer, C. (2006). Inactivation of poliovirus 1 and F-specific RNA phages and degradation of their genomes by UV irradiation at 254 nanometers. *Appl. Environ. Microbiol.* 72, 7671–7677. doi: 10.1128/aem.01106-06

Smirnov, Y. A., Kapitulez, S. P., and Kaverin, N. V. (1992). Effects of UV-irradiation upon Venezuelan equine encephalomyelitis virus. *Virus Res.* 22, 151–158. doi: 10.1016/0168-1702(92)90041-7

Smithyman, K., and Hanawalt, P. C. (1969). *Molecular Photobiology Inactivation and Recovery*. Cambridge: Academic Press.

Stefano, D. R., Burgio, G., Ammatuna, P., Sinatra, A., and Chiarini, A. (1976). Thermal and ultraviolet inactivation of plaque purified measles virus clones. *G. Batteriol. Virol. Immunol.* 69, 3–11.

Thompson, S. S., Jackson, J. L., Suva-Castillo, M., Yanko, W. A., El Jack, Z., Kuo, J., et al. (2003). Detection of infectious human adenoviruses in tertiary-treated and ultraviolet-disinfected wastewater. *Water Environ. Res.* 75, 163–170. doi: 10.2175/106143003x140944

Thurston-Enriquez, J. A., Haas, C. N., Jacangelo, J., Riley, K., and Gerba, C. P. (2003). Inactivation of feline calicivirus and adenovirus type 40 by UV radiation. *Appl. Environ. Microbiol.* 69, 577–582. doi: 10.1128/aem.69.1.577-582.2003

United States Environmental Protection Agency [USEPA] (2020). *List N: Disinfectants for Use Against SARS-CoV-2*. Available online at: https://www.epa.gov/pesticide-registration/list-n-disinfectants-use-against-sars-cov-2 (accessed June 12, 2020).

van Doremalen, N., Bushmaker, T., Morris, D. H., Holbrook, M. G., Gamble, A., Williamson, B. N., et al. (2020). Aerosol and surface stability of SARS-CoV-2 as compared with SARS-CoV-1. *N. Engl. J. Med.* 382, 1564–1567.

von Brodorotti, H. S., and Mahnel, H. (1982). Comparative studies on susceptibility of viruses to ultraviolet rays. *Zentralbl. Veterinarmed. B* 29, 129–136. doi: 10.1007/978-1-4615-6693-9_3

Walker, D. I., Cross, L. J., Stapleton, T. A., Jenkins, C. L., Lees, D. N., and Lowther, J. A. (2019). Assessment of the Applicability of capsid-integrity assays for detecting infectious norovirus inactivated by heat or UV irradiation. *Food Environ. Virol.* 11, 229–237. doi: 10.1007/s12560-019-09390-4

Wang, D., and Tian, P. (2013). Inactivation conditions for human norovirus measured by an in situ capture-qRT-PCR method. *Int. J. Food Microbiol.* 172, 76–82. doi: 10.1016/j.ijfoodmicro.2013.11.027

Weiss, M., and Horzinek, M. C. (1986). Resistance of Berne virus to physical and chemical treatment. *Vet. Microbiol.* 11, 41–49. doi: 10.1016/0378-1135(86)90005-2

Widdowson, M. A., Sulka, A., Bulens, S. N., Beard, R. S., Chaves, S. S., Hammond, R., et al. (2005). Norovirus and foodborne disease, United States, 1991–2000. *Emerg. Infect. Dis.* 11, 95–102. doi: 10.3201/eid1101.040426

Wiedenmann, A., Fischer, B., Straub, U., Wang, C. H., Flehmig, B., and Schoenen, D. (1993). Disinfection of hepatitis A virus and MS-2 coliphage in water by ultraviolet irradiation: comparison of UV-susceptibility. *Water Sci. Technol.* 27, 335–338. doi: 10.2166/wst.1993.0370

Wilson, B. R., Roessler, P. F., van Dellen, E., Abbaszadegan, M., and Gerba, C. P. (1992). "Coliphage MS2 as a UV water disinfection efficacy test surrogate for bacterial and viral pathogens," in *Proceedings of the AWWA Water Quality Technology Conference*, Toronto, ON.

Woo, P. C., Huang, Y., Lau, S. K., and Yuen, K. Y. (2010). Coronavirus genomics and bioinformatics analysis. *Viruses* 2, 1804–1820. doi: 10.3390/v2081803

World Health Organization [WHO] (2020a). *Coronavirus Disease 2019 (COVID-19) Situation Report-143*. Available online at: https://www.who.int/docs/default-source/coronaviruse/situation-reports/20200611-covid-19-sitrep-143.pdf?sfvrsn=2adbe568_4 (accessed June 12, 2020).

World Health Organization [WHO] (2020b). *Report of the WHO-China Joint Mission on Coronavirus Disease 2019 (COVID-19)*. Available online at: https://www.who.int/publications/i/item/report-of-the-who-china-joint-mission-on-coronavirus-disease-2019-(covid-19) (accessed April 10, 2020).

Zavadova, Z., and Libikova, H. (1975). Comparison of the sensitivity to ultraviolet irradiation of reovirus 3 and some viruses of the Kemerovo group. *Acta Virol.* 19, 88–90.

Zhu, N., Zhang, D., Wang, W., Li, X., Yang, B., Song, J., et al. (2020). A novel coronavirus from patients with pneumonia in China, 2019. *N. Engl. J. Med.* 382, 727–733.

Conflict of Interest: The authors declare that the research was conducted in the absence of any commercial or financial relationships that could be construed as a potential conflict of interest.